FREQUENCY OFFSET CORRECTION IN A SOFTWARE DEFINED HIPERLAN/2 DEMODULATOR USING PREAMBLE SECTION A

L.F.W. van Hoesel, F.W. Hoeksema, R. Schiphorst, V.J. Arkesteijn, C.H. Slump

University of Twente, Department of Electrical Engineering
P.O. box 217 – 7500 AE Enschede – The Netherlands
email: {l.f.w.vanhoesel, f.w.hoeksema, r.schiphorst, v.j.arkesteijn, c.h.slump}@el.utwente.nl

In our Software Defined Radio project we perform a feasibility study of a software defined radio for two communication standards: HiperLAN/2 and Bluetooth. In this paper the Matlab/Simulink implementation of the HiperLAN/2 demodulator for the demonstrator of the project is discussed, with special attention for the frequency offset corrector. This type of correction is necessary to prevent large bit error rates that are caused by inter-subcarrier interference. The method that is proposed in this paper uses preamble section A to estimate the frequency offset. Simulation results for an AWGN channel show that the method is capable of correcting frequency offsets up to the boundary defined in the standard [1]. It was observed that frequency offset correction using only preamble section A is sensitive to –for example– synchronization errors in case real-life analog front-end signals are used.

1 INTRODUCTION

The software defined radio (*SDR*) project [2] at the University of Twente is currently investigating the feasibility of a software defined radio. This is done by developing a demonstrator that is capable of demodulation of two communication standards: HiperLAN/2, a high-speed wireless local area network (*WLAN*) standard and Bluetooth, a low-cost and low-speed personal area network standard. Figure 1 shows the configuration of the communication system in the SDR project (see [3]). For the project an *analog front-end* was designed (see [4]).

In this paper the Matlab/Simulink implementation of the HiperLAN/2 demodulator for the demonstrator of SDR project will be discussed and special attention will be given to distortions in the received signal, that are caused by mismatched mixers in transmitter and receiver.

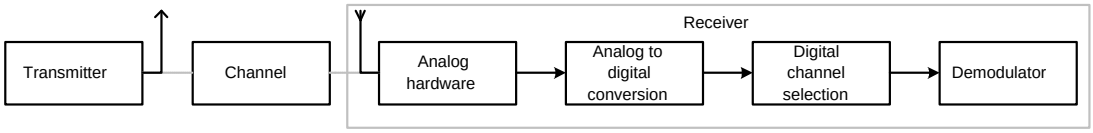

Figure 1: Overview of the SDR projects system configuration

2 HIPERLAN/2

Orthogonal Frequency Division Multiplexing (*OFDM*) has been chosen as modulation technique in HiperLAN/2, because it has a good performance on an indoor radio channel. OFDM is a special kind of *multicarrier modulation*. The modulation technique divides the high data-rate information into several parallel bit streams and each of those bit streams modulates (in groups of 1,2,4 or 6 bits) a separate *subcarrier* using BPSK, QPSK, 16QAM or 64QAM. In this way the radio channel is divided into several independent subchannels, that each carry data at a low rate.

The physical layer of HiperLAN/2 transmits 52 subcarriers in parallel per radio channel. Four of the 52 subcarriers are used to transmit *pilot tones*. These pilot tones assist the coherent demodulation in the receiver. Table 1 gives an overview of the HiperLAN/2 OFDM parameters that will be used throughout this paper.

The transmitted HiperLAN/2 signal $s(t)$ is given by [1] (the carrier frequency in the transmitter is denoted with f_s):

$$s(t) = \sqrt{2} \cdot \Re\left\{ \widetilde{s}(t)\, e^{\jmath 2\pi f_s t} \right\} \tag{1}$$

In which:

$$\widetilde{s}(t) = \sum_{n} \widetilde{s_n}(t) \tag{2}$$

And:

$$\widetilde{s_n}(t) = \begin{cases} \sum_{l=-\frac{N_{ST}}{2}}^{\frac{N_{ST}}{2}} C_{l,n}\, e^{\jmath 2\pi l \Delta_f (t - T_{CP} - nT_S)} & , nT_S \leq t < (n+1)T_S \\ 0 & , \text{else} \end{cases} \tag{3}$$

In equation 3, $C_{l,n}$ denotes the complex symbol value that is transmitted on subcarrier l during OFDM symbol n. In practice a HiperLAN/2 transmitter will work with sampled versions of the baseband signal $\widetilde{s}(t)$ of equation 3. This baseband signal can easily be obtained by taking the *Inverse Fast Fourier Transform* (*IFFT*) of the subcarrier values in a certain OFDM symbol.

Table 1: HiperLAN/2 OFDM parameters

Parameter		Value	
Sampling rate	f_{sample}	20 MHz	($\triangleq 1/T$)
Symbol interval	T_S	$4.0\mu s$	($= 80 \cdot T$)
Useful symbol part duration	T_U	$3.2\mu s$	($= 64 \cdot T$)
Cyclic prefix duration	T_{CP}	$0.8\mu s$	($= 16 \cdot T$)
Number of data carriers	N_{SD}	48	
Number of pilot carriers	N_{SP}	4	
Total number of carriers	N_{ST}	52	
Subcarrier spacing	Δ_f	0.3125 MHz	($= 1/T_U$)

A train of OFDM symbols, containing data of higher protocol layers in HiperLAN/2, is proceeded by a *preamble*. The preamble is a sequence of known OFDM symbols and can consist of three different so called *preamble sections* –named A, B and C–, depending on the type of MAC frame that is transmitted. In [1] the preamble sections are discussed in detail.

3 HIPERLAN/2 DEMODULATOR ARCHITECTURE

The HiperLAN/2 receiver not only has to convert the received signal to data bits by performing the inverse functions of the transmitter, but it also has to try to undo distortions caused by radio channel and hardware of transmitter and receiver. A literature study showed that the following distortions occur in the system depicted in figure 1: 1) Channel effects (noise, interference and delay spread); 2) differences in mix frequencies in transmitter and receiver (the so called *frequency offset*); 3) phase offset in the mixers (causes a so called *common phase offset* to all subcarriers); 4) sample time differences between receiver and transmitter; 5) distortions caused by the digital channel selection filter in the band of interest; 6) phase noise; 7) non-linearity of amplifiers; 8) quantization noise in the analog to digital converter and 9) computational noise.[1]

The first five distortions can be corrected in the demodulator. The other distortions are not correctable against reasonable costs (see [3] and [7]). The demodulator architecture, that is used in the SDR project, is depicted in figure 2. This architecture is implemented in Matlab/Simulink. In this paper *frequency offset correction* using the preamble section A will be discussed in detail. Other implementation aspects and algorithms are described in [3].

[1] See [3], [5], [6], [7], [8], [9] and [10]

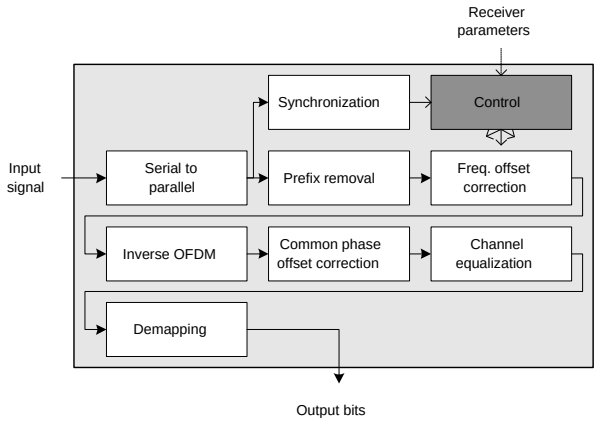

Figure 2: Demodulator part of the receiver; the FFT function is located in the ”Inverse OFDM”-block

4 EFFECTS OF FREQUENCY OFFSET

In this section we will determine the influence of a frequency offset introduced by a mixer mismatch in transmitter and receiver on the performance of the HiperLAN/2 system. Assume that there is a difference f_Δ between the carrier frequency f_s in the transmitter and the carrier frequency in f_r the receiver , then:[2]

$$f_r = f_s + f_\Delta \tag{4}$$

For simplicity we will assume that the channel's transfer function does not distort the received signal and that no noise is present in the system. In this case, the received bandpass signal is given with:

$$r(t) = \sqrt{2} \cdot \Re\{\widetilde{r}(t) e^{\jmath 2\pi f_r t}\} \tag{5}$$

Thus:

$$\widetilde{r}(t) = \widetilde{s}(t)\, e^{-\jmath 2\pi f_\Delta t} \tag{6}$$

From the equation above it can be concluded that a frequency offset can be described at baseband level as a time varying *rotation* of the transmitted complex baseband samples.

At this point we assume that the subcarrier values are retrieved from the sampled version of the baseband signal $\widetilde{r}(t)$ by applying a Discrete Fourier Transformation

[2] Note that this frequency difference is *not* time-dependent. Any time-dependent changes will be represented by *phase noise*.

(*DFT*). We will also assume that the frequency offset f_Δ is smaller than the subcarrier spacing Δ_f. A received subcarrier value $\hat{C}_l$ is given by:

$$\hat{C}_l = \frac{1}{N} \sum_{i=0}^{N-1} \widetilde{r}[i] \; e^{-\jmath 2\pi \frac{il}{N}} \tag{7}$$

With $N = 64$, the number of samples in the useful data part of an OFDM symbol and $\widetilde{r}[i]$ is the sampled received baseband signal at time instances $t = i/f_{sample}$. If equation 6 is substituted in the equation above, this results in:

$$\hat{C}_l = \frac{1}{N} \sum_{i=0}^{N-1} \widetilde{s}[i] \, e^{-\jmath 2\pi \frac{f_\Delta}{f_{sample}} i} \; e^{-\jmath 2\pi \frac{l}{N} i} \tag{8}$$

A single loaded subcarrier value C_γ gives rise to the transmitted complex baseband signal (see also equation 3, $n = 0$):

$$\widetilde{s}[i] = C_\gamma \; e^{\jmath 2\pi \frac{\gamma}{N} i} \; \Big|_{\; i=0 \,\ldots\, N-1} \tag{9}$$

When equation 9 is substituted in equation 8 and the relation $f_{sample} = N \, \Delta_f$ is used, the result is:

$$\hat{C}_l = \frac{1}{N} \sum_{i=0}^{N-1} C_\gamma \; e^{\jmath 2\pi \frac{i}{N} \left(\gamma - l - \frac{f_\Delta}{\Delta_f} \right)} \tag{10}$$

In case no frequency offset is present ($f_\Delta = 0$), the received subcarrier value equals the transmitted subcarrier value $\hat{C}_l = C_\gamma$ only in case $l = \gamma$.

From equation 10 can be concluded that a frequency offset causes *inter-subcarrier interference* (loss of orthogonality). If a frequency offset is present of, for example, $f_\Delta = 1/10 \; \Delta_f = 31.250$ kHz, and $C_\gamma = 1$, the received subcarrier value $\hat{C}_{l=\gamma}$ will be slightly less than the transmitted subcarrier value and some of its energy will flow to neighboring subcarriers (see figure 3a and b).

The HiperLAN/2 standard [1] defines that:

$$\frac{f_c - f_s}{f_c} < 0.002 \;\; \% \tag{11}$$

With f_c the nominal carrier frequency. If we assume an equal demand for f_r compared to f_c, f_Δ may be up to 250 kHz. A quick calculation using equation 10 shows that at this frequency offset, almost all power of a transmitted subcarrier is found in the neighboring subcarrier in the receiver; large bit errors rates will occur. It follows that

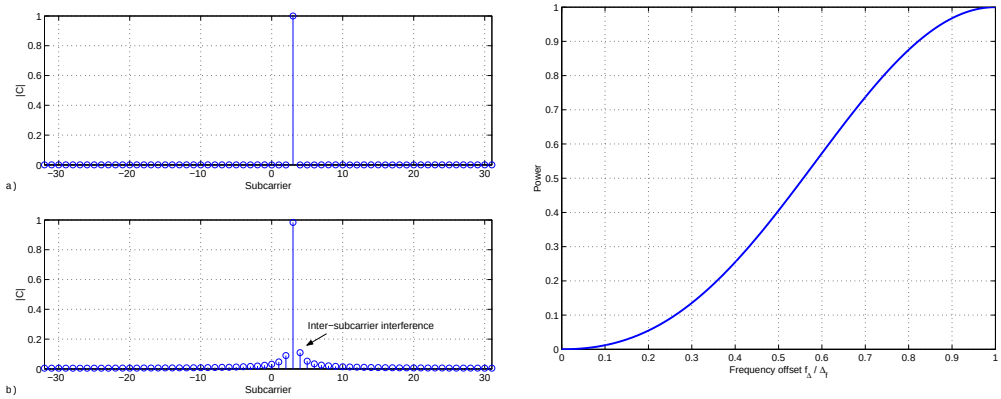

(a) no frequency offset present and (b) a frequency offset of $f_\Delta = 1/10\ \Delta_f = 31.250$ kHz

(c) Influence of frequency offset on neighboring subcarrier in direction of the frequency offset

Figure 3: Effects of frequency offset

the HiperLAN/2 demodulator should try to compensate for frequency offsets.

In figure 3c the (normalized) power that spills into a neighboring subcarrier in the direction of the frequency offset is plotted (see also [9], chapter 21).

5 IMPLEMENTATION OF FREQUENCY OFFSET CORRECTION

The preamble sections are –just like regular OFDM symbols– distorted by a frequency offset. Since the sections contain *known* subcarrier values, the data can be used to measure effects of a frequency offset. We will denote the measured frequency offset by f'_Δ. This measurement should be as close as possible to f_Δ.

There are two approaches to this problem; the frequency offset can be determined in the frequency domain and in the time domain.[3] The frequency domain method is discussed in [3] and uses the results of figure 3c. In our demodulator we choose to implement the time domain method.

We define a vector $\vec{v}_{preamble_A}$ that contains the known sample values of preamble section A. Consider the following definition for the angle Θ between two complex numbers ($a, b \in \mathbb{C}$ and $a, b \neq 0$):

$$\Theta(a,b) \triangleq \arctan\left(\frac{\Re(a)}{\Im(a)}\right) - \arctan\left(\frac{\Re(b)}{\Im(b)}\right) \tag{12}$$

[3] Note that the demodulator exists of two parts: a time domain part and a frequency domain part, since an FFT is used to demodulate the subcarriers (see figure 2).

We will determine the rotation between the *known* sample value in the preamble section and the *received* input sample. Subsequently the slope of the *regression line* of the rotation will be calculated. The regression slope $\dot{\Theta}$ is defined as (see [3]):

$$\dot{\Theta}(\vec{v}_{preamble_A}, \widetilde{r}) = \frac{N \cdot \sum_{i=0}^{N-1} i\,\Theta(\vec{v}_{preamble_A}[i], \widetilde{r}[i]) \;-\; \sum_{i=0}^{N-1} i \cdot \sum_{i=0}^{N-1} \Theta(\vec{v}_{preamble_A}[i], \widetilde{r}[i])}{N \cdot \sum_{i=0}^{N-1} i^2 - \left(\sum_{i=0}^{N-1} i\right)^2} \tag{13}$$

With $N = 64$ is the number of samples that we use, and $\widetilde{r}$ a vector of 64 received baseband samples.

The result of equation 13 is the estimated *rotation per sample*. This value can easily be used to calculate f'_Δ:

$$f'_\Delta = \frac{\dot{\Theta}(\vec{v}_{preamble_A}, \widetilde{r})}{2\pi}\, f_{sample} \tag{14}$$

Note that other distortions can have influence on the frequency offset estimation we calculate (see the list in section 3).

A positive value of f'_Δ implies that it is estimated that $f_r < f_s$ (see equation 4). All input samples, that follow preamble section A, are corrected with:

$$\widetilde{r'}(t) \;\triangleq\; \widetilde{r}(t)\; e^{\jmath 2\pi f'_\Delta t} \;=\; \widetilde{s}(t)\; e^{\jmath 2\pi (f'_\Delta - f_\Delta) t} \tag{15}$$

before further processing.

6 SIMULATION RESULTS

To determine the influence of additive white Gaussian noise (*AWGN*) on the frequency offset estimation and correction, a frequency offset will be introduced to the input of the receiver by multiplying the output of the transmitter with a complex power of e (as in equation 6). The model configuration used for the experiment in this section is shown in figure 4.[4]

In figures 5a and b the BER curves of the experiment discussed above, are depicted for the subcarrier modulation technique 16QAM. Per simulation 10,000 OFDM sym-

[4] The "*ramp*" block of Matlab/Simulink is used to generate the time dependent argument for the complex exponent of e.

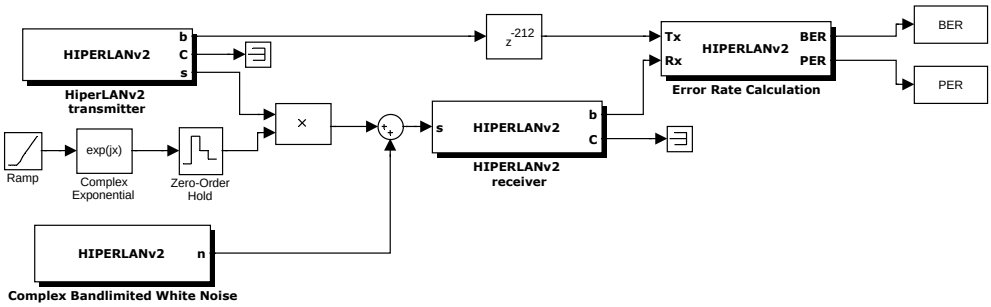

Figure 4: Matlab model for frequency offset simulations

bols were transmitted. The frequency offset in the simulation experiment is changed from $f_\Delta = \Delta_f/5$ to $f_\Delta = \Delta_f$ in steps of $\Delta_f/5$.

From figure 5a, which shows the BER results with the frequency offset correction disabled, can be concluded that frequency offsets up to $f_\Delta = 62.5$ kHz do *not* need to be corrected. For that frequency offset, the inter-subcarrier interference will cause about 5% of the power of a neighboring subcarrier to spill into a subcarrier (see figure 3c), apparently without consequences for the BER. Other frequency offsets cause BERs of ≈ 0.5.

Figure 5b shows the results when the frequency offset correction is enabled. The frequency offset corrector can correct all tested frequency offsets, except for $f_\Delta = \Delta_f$. Note that the maximum allowed frequency offset in the HiperLAN/2 system is 250 kHz. The frequency offset results stay within 1.5 dB of their theoretical expected value.

In figure 6 the standard deviation of the frequency offset f_Δ minus the estimated frequency offset f'_Δ is plotted. As can be seen from figure 5b, the system was not able to correct the frequency offset for $f_\Delta = \Delta_f = 312.5$ kHz. In this case the frequency offset results in a 2π phase shift in 64 samples (the useful data part). As the standard deviation in this case is comparable to the standard deviations depicted in the other curves, it must be concluded that other moments of the distribution (the mean comes to mind) are responsible for the large BERs.

In interpreting the curves for $f_\Delta = 62.5$ kHz and $f_\Delta = 250$ kHz one would expect a similarity in shape because of symmetry considerations. In the figure we do not see this. We think that this is caused by the implementation of equation 12: in case the rotation per useful data part is near 2π, even small noise disturbances may cause a modulo -2π operation, influencing the regression.

The last two curves, for $f_\Delta = 125$ kHz and $f_\Delta = 187.5$ kHz, show a similar shape, as can be expected from symmetry considerations. The modulo-problem does not seem to occur. In the $f_\Delta = 187.5$ kHz case, the rotation per sample is larger than

in the $f_\Delta = 125\,\text{kHz}$ case and is hence estimated more accurately, for a given noise power.

7 CONCLUSION AND DISCUSSION

From the analysis in section 4 and from the simulation results in figure 5a it can be concluded that a frequency offset corrector is necessary in a HiperLAN/2 demodulator. In this paper a method for estimation of the frequency offset is proposed that uses only preamble section A. Simulation results of an AWGN environment showed that this method is capable of correcting frequency offsets up to 250 kHz, the frequency offset boundary that follows from the HiperLAN/2 physical layer definition in [1].

An analog front-end has been designed for our SDR demonstrator (see [4]). Preliminary measurement results with this analog front-end have shown that the frequency offset corrector in the demodulator does not always function correctly. We believe this to be caused by the implementation of equation 12 in the estimator and fact that preamble section A is the first section of a burst and hence not all other distortions are yet estimated and corrected, because they are estimated using other preamble sections.

Further research has to be done into the influence of other signal distortions on our method of frequency offset correction and to the divisions of preamble sections among the various other corrections necessary in a HiperLAN/2 demodulator.

REFERENCES

[1] ETSI. *Broadband Radio Access Networks (BRAN); HIPERLAN Type 2; Physical (PHY) layer*. 2001. ETSI TS 101 475 V1.2.2 (2001-02).

[2] `http://nt5.el.utwente.nl/sdr`.

[3] L.F.W. van Hoesel. *Design and implementation of a software defined HiperLAN/2 physical layer model for simulation purposes*. Master of Science Thesis, Universiteit Twente, EL SAS 032 N 02, 2002.

[4] V.J. Arkesteijn, E.A.M. Klumperink, and B. Nauta. *An Analogue Front-End Test-Bed for Software Defined Radio*. MMSA, 2002.

[5] S. Armour, M. Butler, and A. Doufexi et al. *A Comparison of the HiperLAN/2 and IEEE 802.11a Wireless LAN Standards*. IEEE Communications Magazine, pages 172–180, May 2002.

[6] J. Medbo and P. Schramm. *ETSI EP BRAN3ERI085B; Channel Models for HiperLAN/2 in Different Indoor Scenarios*. March 1998.

[7] S.A. Fechtel, G. Fock, H. Meyr, and M. Speth. *Optimum receiver design for wireless broad-band systems using OFDM - Part I*. IEEE Transactions on Communications, Vol 47 No. 11 p. 1668-1677, 1999.

[8] R. van Nee. *OFDM for wireless multimedia communications*. Artech House Publishers England, 2000.

[9] L. Hanzo, T. Keller, and W. Web. *Single- and Multi-carrier Quadrature Amplitude Modulation; Principles and Applications for Personal Communications, WLANs and Broadcasting*. Wiley, U.S.A., 2000.

[10] L.W. Couch. *Digital and analog communication systems*. Prentice Hall, U.S.A., fifth edition, 1997.

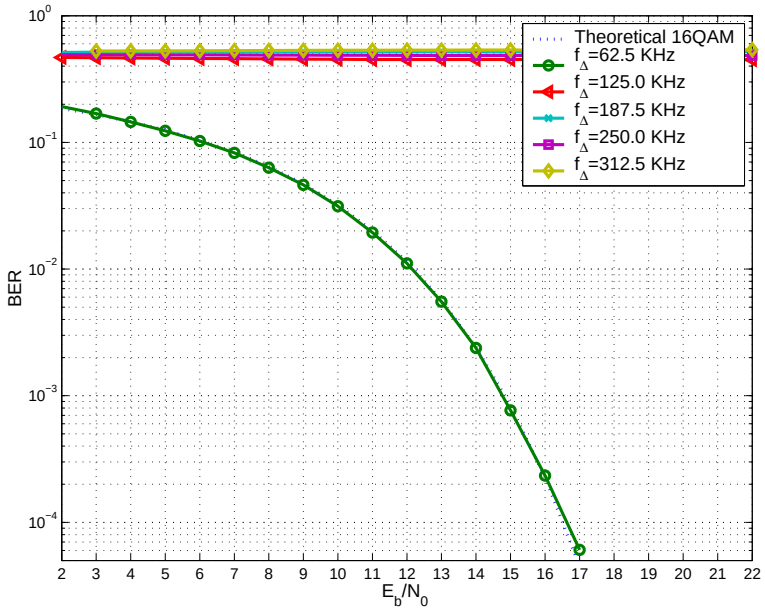

(a) The frequency offset correction is *not* active

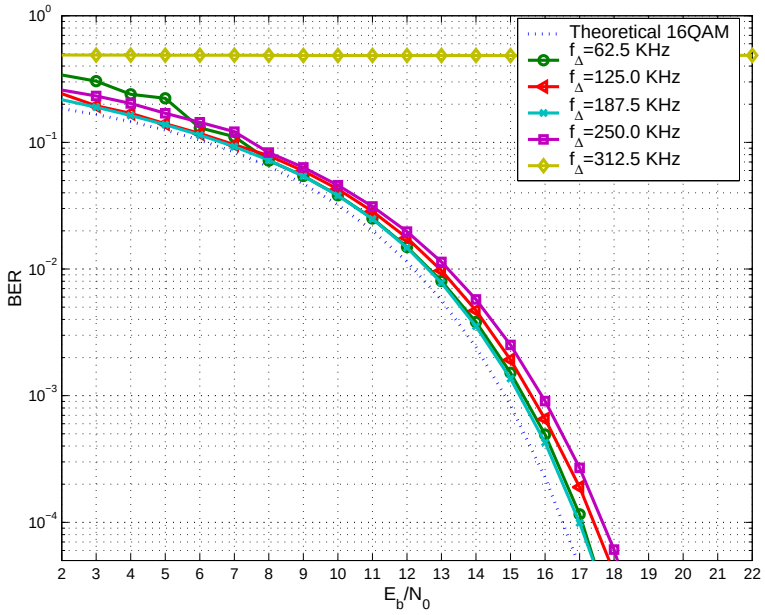

(b) The frequency offset correction is active

Figure 5: Frequency offset simulation results

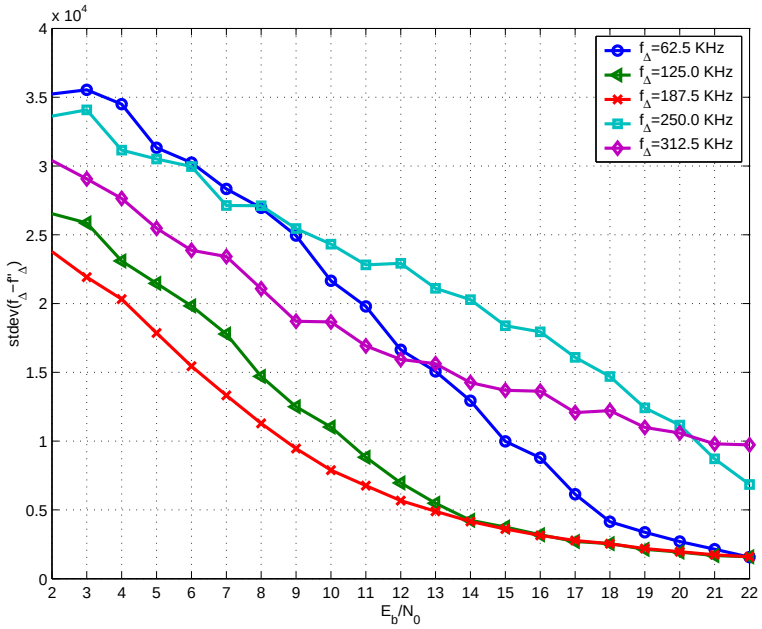

Figure 6: Standard deviation between the frequency offset f_Δ and the estimated frequency offset f'_Δ